Zeolite-catalyzed one-pot sucrose-to-HMF transformation: Ge outperforms Sn, Zr, and Al sites

Poonam Rani[#], Jin Zhang[#], Yuqi Zhang, Maksym Opanasenko, and Mariya Shamzhy*

Department of Physical and Macromolecular Chemistry, Faculty of Science, Charles University, Hlavova 8, 12843 Prague 2, Czech Republic

[#]Equal contribution

Abstract

The conversion of renewable compounds to versatile platform molecules over environmentally friendly heterogeneous catalysts is a major challenge. Zeolites stand as active, selective, and reusable solid catalysts for various acid-catalyzed reactions involved in the one-pot cascade transformation of polysaccharides to 5-hydroxymethylfurfural (HMF), a platform molecule opening the way to various valuable chemicals. However, the acidity-performance relationships of zeolite catalysts in HMF synthesis have not been fully elucidated. Here, we have addressed the effect of acid site strength of zeolite catalysts in sucrose-to-HMF transformation by comparing the performance of conventional Al-containing zeolite with that of Sn-, Zr-, and Ge-containing catalysts of the same structure. Weak Ge-associated acid sites were found to outperform stronger Sn, Zr, and Al acid centers in terms of activity and selectivity, while the optimization of germanosilicate catalyst structure (Ge-IWW vs. Ge-UTL or Ge-*CTH) enabled to achieve the yield of targeted HMF comparable to or even exceeding the values previously reported for homogeneous or heterogeneous catalysis (54 % after 3 h at 120 °C). The results of this study highlight zeolites with uncharacteristic chemical compositions as active, selective, and reusable catalysts for highly demanding applications in biomass valorization.

Keywords: germanosilicate; zeolites; acid catalysis; biomass; sucrose; hydroxymethylfurfural

Introduction

Regarding utilization of catalysis for emerging applications, the transformation of biomass into valuable products is of utmost importance. The recent array of research efforts has quantified biomass to be abundantly available alternative renewable resources. Enormous efforts are being made for catalytic transformation of renewable biomass (cellulose, carbohydrates, etc.) into fuels and value-added chemicals [1]. Among the biomass-derived platform chemicals, 5-hydroxymethylfurfural (HMF) is considered a versatile building block that can undergo oxidation or reduction to form the valuable derivatives, generally used as precursors in the polymer industry and in the production of liquid fuels [2].

Most of the catalysts used for the transformation of biomass-derived polysaccharides, such as sucrose into HMF, have the same catalytic mechanism (Scheme 1) [3]. Initially, Brønsted acid-catalyzed hydrolysis of sucrose to hexoses (glucose and fructose) occurs. It is followed by the Lewis acid-catalyzed isomerization of glucose to fructose and a subsequent dehydration reaction. Glucose can undergo direct Brønsted acid-catalyzed dehydration to HMF, but the rate of this process was reported to be low [4]. Catalysts in sucrose-to-HMF transformation influence the reaction rate of different steps and in this way alter the rate of side-product formation, such as levulinic and formic acids. The by-products generated along with HMF pose a significant obstacle to scaling up the process, leading to reduced HMF selectivity and yield. Humins are formed predominantly at elevated temperatures, while levulinic acid is produced as a rehydration byproduct from HMF [5].

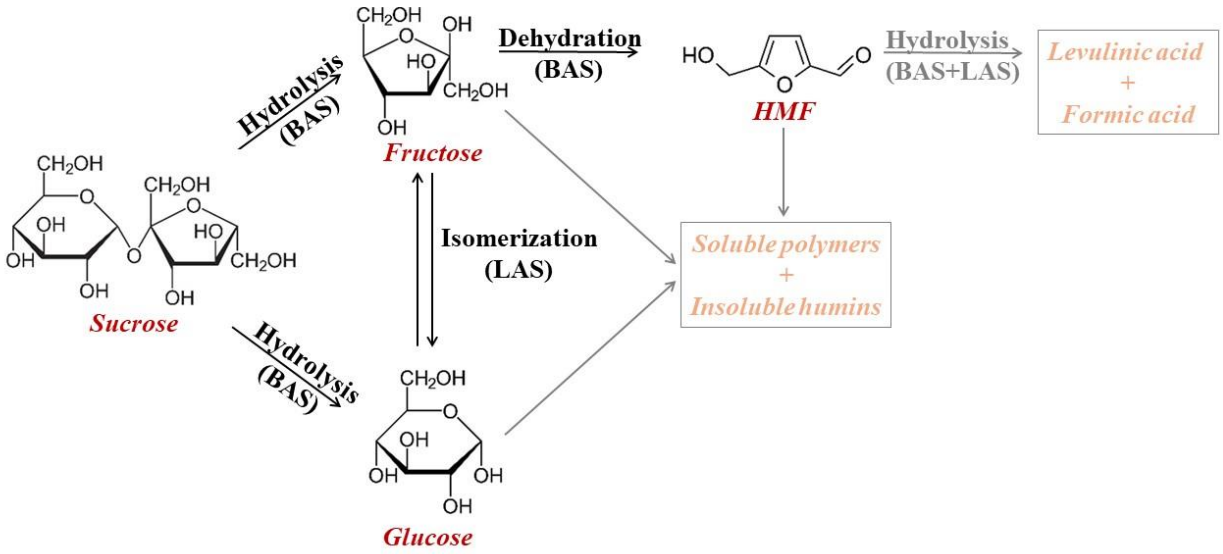

Scheme 1 Schematic presentation of the multistep transformation of sucrose to HMF through hexoses.

In recent decades, several homogeneous and heterogeneous catalysts have been explored for the HMF synthesis. Using homogeneous catalysts, such as mineral and organic acids, for the synthesis of HMF suffers from costly separation and corrosion issues, while heterogeneous catalysts overcoming these limitations have better application prospects. Currently, a variety of heterogeneous catalysts have been studied for the preparation of HMF, including zeolites, metal oxides, heteropoly acids, metal-organic frameworks, etc. [6].

Zeolites have high thermal stability, adjustable acidity, and tunable structural characteristics (crystal size and shape, pore size distribution), all having a major impact on the reaction pathway as well as the product distribution [7]. The rational fine-tuning of zeolite catalyst characteristics may open the way to maximize their performance in HMF synthesis. Classical zeolites (aluminosilicates) as well as four-valent element-substituted zeolites possess acid sites of different natures required for the sucrose-to-HMF transformation. In particular, 10-ring MFI and 12-ring Beta zeolite catalysts were found to be promising candidates in the majority of studies [8-10]. Sn-zeolites have been explored in isomerization and in the glucose-to-HMF transformation [11, 12]. Monosaccharides like fructose and glucose are frequently employed as model molecules in the synthesis of HMF using zeolite catalysts, yielding high HMF yields [13]. The more appealing one-pot conversion of polysaccharides, such as sucrose, and actual biomass into HMF is less studied preventing the design of active and selective zeolite catalysts for sustainable HMF synthesis.

Until, now, more than 250 zeolite frameworks have been reported and classified based on pore size (8-, 10- 12- and >12-ring), crystal structure, and elemental composition [14]. Along with the pore system, the presence of heteroatoms in the silica framework is decisive for the catalytic activity of the zeolite. In addition to the aluminum mentioned above, other elements such as zinc, titanium, tin, boron, and germanium can also substitute silicon atoms [15]. Among them, aluminosilicate zeolites rule the bulk and fine chemical synthesis due to their high thermostability, acidity, and shape selectivity, while the applications of other heteroatom-containing zeolites are still limited. Recently, germanosilicates have attracted a lot of attention due to their potential ability to provide new zeolite framework topologies [16-19]. Synergetic effect of Ge species in the synthesis gel provides new zeolite structures which are difficult to obtain from aluminosilicate or silicate systems. The chemical properties of the resulting zeolites were further engineered by the substitution of Ge for Sn, Zr, Al and Ti *via* post-synthesis substitution, which provides the tunable acidity [20-26]. The mentioned possibilities (new structures, easily variable chemical compositions) provided by germanosilicate zeolites and their derivatives offer further tools for optimization of numerous catalytic processes being a part of biomass transformation chemistry.

This study aimed to address the structure-acidity-performance relationships in zeolite-catalyzed one-pot cascade sucrose-to-HMF transformation. For that, we have designed and synthesized a series of large-pore IWW zeolites containing Ge, Al, Sn, and Zr acid sites, as well as Ge-containing zeolites of different structures (IWW, UTL, and *CTH). The catalysts were comprehensively characterized using X-ray diffraction, nitrogen physisorption, scanning electron microscopy, and FTIR spectroscopy of adsorbed pyridine and tested in sucrose-to-HMF transformation. The

obtained results are expected to provide a guide for optimizing the zeolite catalyst properties to maximize the yield of HMF synthesis via a given catalytic route.

Experimental section

Catalysts preparation

IWW zeolite catalysts with variable chemical composition. Germanosilicate Ge-IWW zeolite was prepared according to Ref. [27] using 1,5-bis(methylpyrrolidinium) pentane dihydroxide ($MPP(OH)_2$) as the structure-directing agent. For that, the appropriate amount of GeO_2 was dissolved in 1M aqueous solution of $MPP(OH)_2$, followed by the addition of TEOS under vigorous stirring. After evaporating excess water/ethanol, the reaction suspension with the composition of 0.67 SiO_2 : 0.33 GeO_2 : 0.25 $MPP(OH)_2$: 15 H_2O was heated in a Teflon stainless steel autoclave at 175 ºC for 7 days under static conditions. The solid product was recovered by filtration, washed with deionized water, dried at 60 ºC overnight, and further calcined at 580 ºC for 6 h under air flow. Ge-IWW possesses a Si/Ge molar ratio of 5 according to the ICP-MS analysis.

Sn- and Al-IWW were prepared by post-synthesis of Ge-IWW, as described in Ref. [28] (Scheme 2). For that, Ge-IWW was initially hydrolysed with water at 25 °C for 16 h, while isolating the solid product by filtration. This procedure was repeated 3 times to obtain the degermanated IWW zeolite with a Si/Ge molar ratio of 70 according to the ICP-MS analysis.

For the preparation of Al-IWW, degermanated Ge-IWW was treated with 1M aqueous solution of $Al(NO_3)_3$ (1g zeolite /100ml solution) at 95 °C for 96 h. For Sn-IWW preparation, degermanated Ge-IWW was first activated at 450 °C for 4 h to remove the adsorbed water and then treated with 0.45 M $SnCl_4$ solution in heptane (1g zeolite /100ml solution) at 95 °C for 96 h under nitrogen atmosphere. Solid products were isolated by filtration, washed with deionized water (for Al-IWW) or heptane (for Sn-IWW), dried at 60 ºC overnight, and further calcined at 450 ºC for 4 h.

Zr-IWW was prepared using the vapour-state ion-exchange method [21] in a quartz crucible with self-sealing. Firstly, 0.25 g of degermanated Ge-IWW was placed in the quartz cap of the crucible and activated at 450 ºC for 4 h to remove adsorbed water. After the temperature decreased to 250 ºC, the quartz tube with 0.5 g of anhydrous $ZrCl_4$ powder was placed in the oven. The zeolite sample and metal precursor were separated with a thermally stable borosilicate glass filter, which can withstand a temperature of 500 ºC. The vapor-phase treatment of a zeolite took place at 300 ºC for 10 h at a rate of 1 ºC·min^{-1}. Finally, the glass filter and the quartz tube were removed from the oven and the sample was further calcined at 550 ºC for 6 h to ensure completeness of Zr incorporation.

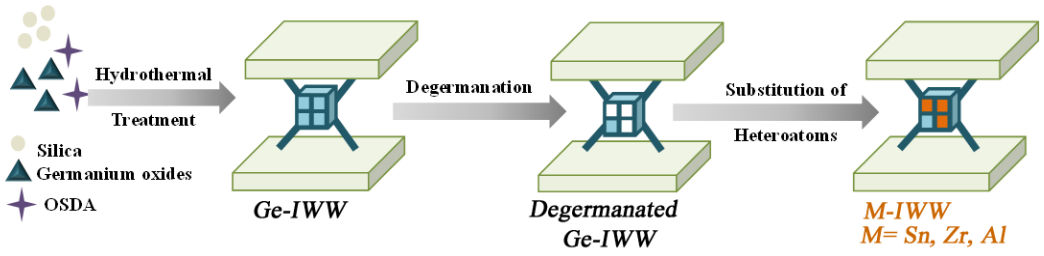

Scheme 2: Synthesis and post-synthesis modification of Ge-IWW zeolite for the preparation of catalysts with variable active site nature.

Germanosilicate zeolite catalysts with variable structure. Ge-UTL was prepared according to Ref. [29] using (6R,10S)-6,10-dimethyl-5-azoniaspiro[4,5]decane hydroxide (DMAD(OH)) as a structure-directing agent. Germanium oxide (IV) and fumed silica were used as the sources of framework-building elements. The reaction suspension with the composition of 0.8 SiO_2 : 0.4 GeO_2 : 0.65 DMAD(OH) : 30 H_2O was crystallized in a Teflon stainless steel autoclave at 175 ºC under agitation for 7 days. It was followed by filtration, washing with deionized water, drying at 60 ºC overnight, and calcination at 550 ºC for 6 h in air flow. Ge-UTL has a Si/Ge molar ratio of 4 according to the ICP-MS analysis.

Ge-*CTH was prepared according to Ref. [30] using 1,2-dimethyl-3-(3-methylbenzyl)imidazolium hydroxide (DMBI(OH)) as a structure-directing agent. Germanium oxide (IV) and TEOS were used as the sources of framework-building elements. The reaction suspension with the composition of 0.8 SiO_2: 0.2 GeO_2: 0.5 DMBI: 0.5 HF: 10 H_2O was crystallized in a Teflon stainless steel autoclave at 160 ºC under static conditions for 30 days. The solid product was recovered by filtration, washed with deionized water, dried at 60 ºC overnight, and calcined at 580 ºC for 6 h in air flow. Ge-*CTH has a Si/Ge molar ratio of 4 according to the ICP-MS analysis.

Characterization

X-ray diffraction (XRD) patterns were recorded in the 2θ range of 5 – 40° with a scan speed of 0.25° (2θ)/min on a Bruker AXS D8 Advance diffractometer with a Vantec-1 detector in Bragg-Brentano geometry using Cu Kα radiation (λ = 1.5405Å).

Nitrogen sorption measurements were performed at -196 °C on 3Flex (Micromeritics) static volumetric apparatus. Before measurement, the samples were outgassed at 300 °C for 8 h with a turbo molecular pump at $p < 10^{-2}$ Pa. The BET method was applied to calculate the specific surface area in the relative pressure range (p/p0) of 0.05 ~ 0.20. The micropore volume (Vmicro)[46] was evaluated using the t-plot method and the NLDFT model [31].

Scanning electron microscopy (SEM) measurements were carried out on a TESCAN Vega microscope to investigate the morphology of the samples.

Elemental analysis was performed by inductively coupled plasma mass spectrometry (ICP-MS; ThermoScientific iCAP 7000). A closed vessel containing a mixture of 50 mg of zeolite, 1.8 ml of HF, 5.4 ml of HCl, and 1.8 ml of HNO_3 was placed in a microwave oven to dissolve the zeolite. To complex the surplus HF after cooling down, 13.5 ml of H3BO3 was added and reheated in the microwave oven.

The acid site nature in designed zeolites was investigated by FTIR spectroscopy of adsorbed pyridine (FTIR-Py). For this purpose, the zeolites were pressed into self-supporting wafers with a density of ~10 mg/cm^2 and *in situ* activated at 450 °C and p = 5x10^{-5} Torr for 4 h. An excess of pyridine (Py) was adsorbed at 25°C for 20 minutes, followed by 20-minute desorption at the same temperature. Py thermodesorption was performed for 20 min at 25, 50, 75, 100, 120 and 150 °C for germanosilicate zeolite catalysts, Sn-IWW and Zr-IWW samples, and at 150, 250, 350, 450 °C for Al-IWW zeolite. FTIR spectra were recorded using a Nicolet iS50 spectrometer with a transmission MTC/B detector with a resolution of 4 cm^{-1} by collecting 128 scans for a single spectrum at room temperature. The spectra were processed using the Omnic 8.2 program (Thermo Scientific). For baseline correction, the spectrum of activated sample was subtracted from the spectra collected after Py adsorption/desorption. The number of Brønsted acid sites was estimated based on the integral intensity of the band at 1545 cm^{-1}. The number of Lewis acid sites was estimated from the integral intensities of the bands at 1454 cm^{-1} (for Al-IWW) and at 1608 - 1611 cm^{-1} (for Ge-IWW, Sn-IWW, Zr-IWW, Ge-UTL and Ge-*CTH zeolites). To determine the area of the peak characteristic for coordinatively bonded (1608 - 1611 cm^{-1}) and H-bonded (1596 cm^{-1}) Py, the resulting spectral curve was fitted using the Gaussian line shape. IR peak centers were fixed within ±5 cm^{-1}, and the full widths at half maxima were constrained between 5 cm^{-1} and 20 cm^{-1}. To estimate the relative strength of the Lewis acid sites in the designed catalysts, the intensity of the characteristic bands at 200 °C was related to those at 25°C as follows:

$$(1)\ BAS_{strong} = \frac{A_{1545}^{200^oC}}{A_{1545}^{25^oC}} \cdot 100\ [\%]$$

$$(2)\ LAS_{strong} = \frac{A_{1608}^{200^oC}}{A_{1608}^{200^oC}} \cdot 100\ [\%]$$

Catalytic experiment

Before catalytic tests, 50 mg of the zeolite catalyst were activated at 450 °C for 4 h. Catalytic experiments were carried out at 120 °C in a batch reactor using a multi-experiment workstation StarFish^{TM}. Typically, sucrose aqueous solution (10 wt. %, 1 mmol of sucrose) and dimethylsulfoxide (DMSO, 5 mL) were charged into a three-neck flask equipped with a thermometer and a condenser. An activated catalyst was added to the flask when the required temperature was reached.

For the recycling experiment, the catalyst was separated from the reaction mixture by centrifugation and washed several times with EtOH and acetone. The recovered catalyst was dried at 60 °C overnight and then activated at 450 °C for 4 h before the next catalytic run.

The reaction mixture was collected periodically, centrifuged to separate the liquid fraction, and analysed using the ^{1}H NMR spectroscopy and HPLC to determine sucrose conversion and HMF selectivity, respectively. ^{1}H NMR spectroscopy was performed on a Bruker Advance III Ultra Shield 500 MHz spectrometer operating at 500.13 MHz for ^{1}H NMR using DMSO-d6 as a solvent. HPLC was performed using a Waters Acquity UPLC H single-bond Class system (Waters, Milford, USA) equipped with a photodiode array detector (960 UV, 280 nm). Empower 3 software was used for system control, data acquisition, and results processing. Separation was carried out with a 5 µm Zorbax Eclipse XDB-C18 column of 4.6 x 150 mm (Waters, Milford, USA), using 20:80 v/v methanol:water as the mobile phase at a flow rate of 0.6 ml min^{-1} and a column temperature of 35 ° C.

Results and discussion

Physico-chemical characteristics of zeolite catalysts

All members of the designed set of IWW zeolite catalysts with variable chemical composition were of high phase purity as their powder XRD patterns showed the diffraction lines characteristic of IWW framework and no signs of admixed phases (Figure S1) [27]. Al-IWW, Sn-IWW and Zr-IWW showed the same position of characteristic diffraction lines as the parent Ge-IWW zeolite (e.g, 4.20 (d_{200}), 6.98 (d_{001}), 8.00 (d_{210}), 8.34 (d_{400}) 9.30 (d_{310}), 10.64 (d_{211}) 2θ, etc.), but with modified relative intensities. The change in relative intensities of diffraction lines upon post-synthesis substitution of Ge for different metals evidences the alteration of the material density upon incorporation of Al, Sn, and Zr atoms into the framework positions.

Ge-IWW crystallized as small rectangular crystals with particle size ≤1 µm which are somewhat agglomerated (Figure 1). Heteroatom substitution in the IWW framework did not cause a significant change in the morphology of the crystals but influenced the size of their aggregates. Al-IWW possessed larger assembles of crystals (1 – 2 µm) compared to Sn, Zr-substituted analogues (< 1 µm) or initial Ge-IWW zeolite.

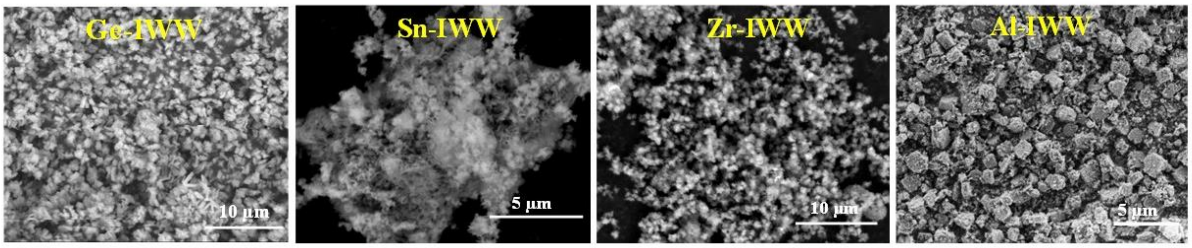

Figure 1: SEM images of the IWW zeolite catalysts under study.

Nitrogen physisorption results reveal the microporous character of IWW zeolite catalysts, as the respective adsorption isotherms of all Ge-IWW, Al-IWW, Sn-IWW, and Zr-IWW show a rapid increase in the adsorbed amount up to the limit value at quite low $p/p_0 < 0.03$ (Figure S2). The subsequent uptake of nitrogen at $p/p_0 > 0.5$ arising from adsorption in intercrystalline voids is especially pronounced for Sn-IWW and Al-IWW in accordance with their relatively small crystal sizes. Analysis of the micropore adsorption capacity (Table 1) showed that Sn-, Zr-, Al-substituted IWW catalysts had similar (Al-IWW) or slightly lower (Sn- and Zr-IWW) micropore volumes compared to those of the parent Ge-IWW. These results may be explained by the increase in the density of the material after the substitution of Ge atoms with metal atoms.

Table 1: Chemical composition, textural and acidic properties of IWW zeolite catalysts under study

Material	Chemical composition[a]		V_{micro} ($cm^3 \cdot g^{-1}$)[b]	S_{BET} ($m^2 \cdot g^{-1}$)[b]	Strong acid sites (%)[c]	
	Si/Ge	Si/Me			Brønsted	Lewis
Ge-IWW	5	-	0.16	444	0 (0.07 mmol/g)	0
Zr-IWW	71	13	0.10	254	No	40
Sn-IWW	70	33	0.11	361	No	53
Al-IWW	70	25	0.14	411	100 (0.10 mmol/g)	100

[a] – based on ICP-MS analysis;
[b] – based on nitrogen physisorption;
[c] – based on FTIR spectroscopy of adsorbed pyridine

Variation of the framework elements responsible for the acidic properties of the zeolites (Ge, Al, Zr, Sn) is expected to influence the nature and strength of the acid centers, expected to directly affect the activity and selectivity of the designed materials in the sucrose transformation [5, 6, 13]. Therefore, the acidity of the catalysts was investigated using infrared spectroscopy after adsorption of pyridine as base probe molecule (Py-FTIR). Figure S3 shows the Py-FTIR spectra of IWW zeolite catalysts of different chemical compositions. All Ge-, Zr-, Sn- and Al-IWW catalysts contain Lewis acid sites, as follows from the presence of characteristic bands of υ_{8a}=1611 and υ_{19b}

=1453 cm^{-1}. In addition to the characteristic bands of the Lewis acid sites, Al-IWW demonstrates apparent Brønsted acidity (υ_{8a} =1637 and υ_{19b} =1545 cm^{-1}), while such a feature was less pronounced for Ge-IWW and was not observed in both Zr-IWW and Sn-IWW zeolites [32]. Along with the characteristic peaks of pyridine adsorbed on acid sites, spectra of all materials contained bands related to the hydrogen bonded pyridine (υ_{8a}=1596 and υ_{19b}=1443 cm^{-1}) as well as physisorbed Py (υ_{8a}=1577 and υ_{19b}=1438 cm^{-1}). Furthermore, the relative strength of the observed acid centers was analyzed by pyridine thermodesorption (Figure 2, Table 1). The fraction of strong Lewis acid sites decreased in the following sequence of the catalysts: Al-IWW >> Sn-IWW > Zr-IWW >> Ge-IWW. In turn, Ge-IWW featured much weaker Brønsted acid sites compared to Al-IWW (Table 1). The obtained results were in line with previous reports on acid site strength in zeolites [32-34].

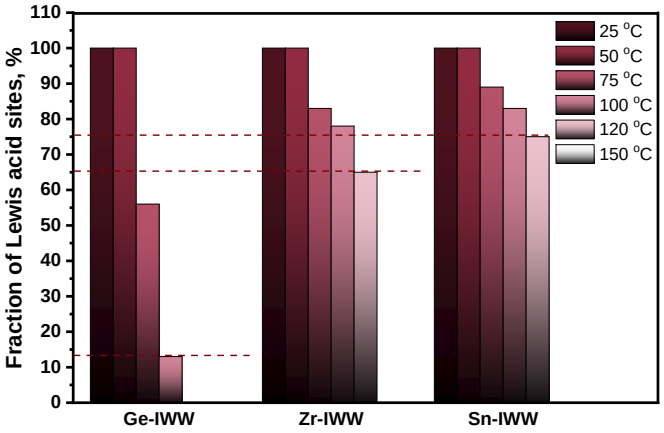

Figure 2: Fraction of Lewis acid sites (in %) in Ge-, Zr-, and Sn-IWW zeolite catalysts that retain adsorbed pyridine at variable temperatures.

According to their characteristics, the prepared IWW zeolite catalysts with variable chemical composition were qualified as a representative set of materials, appropriate for analyzing the influence of the nature and strength of acid centers on the outcome of sucrose-to-HMF transformation with an ultimate goal to assess the optimal catalyst characteristics to maximize the yield of HMF.

3.2. Catalytic activity

No sucrose conversion was observed in the blank experiment without catalysts, while all characteristic peaks of HMF were observed in the ^{1}H NMR spectra at different reaction times when zeolite catalysts were introduced to the reaction system (Figure S4). Under selected reaction conditions, the optimal reaction time was found to be 3 h (Figure S5), as the HMF concentration in the product mixture decreased at prolonged times due to the subsequent conversion of HMF into side products, such as decomposition to levulinic and formic acids or condensation.

The conversion of sucrose over different IWW zeolite catalysts after 3h was in the range 64 – 73 %, while their selectivities to HMF and the yield of the targeted product differ significantly (Figure 3). Notably, monofunctional Lewis acid Sn- and Zr-IWW catalysts and weakly acidic Brønsted/Lewis Ge-IWW zeolite showed higher selectivity to HMF (72 – 80 % selectivity at 60 % conversion) than the strongly acidic Brønsted/Lewis Al-IWW catalyst (70 % selectivity). In general, in the range of IWW zeolite catalysts, the yield of the targeted HMF decreased with increasing acid site strength due to the enhanced formation of by-products from HMF in the following sequence: Ge-IWW > Zr-IWW > Sn-IWW > Al-IWW. (Fig. 7b). The result is consistent with the formation of a higher fraction of side products instead of HMF on stronger acid sites [35].

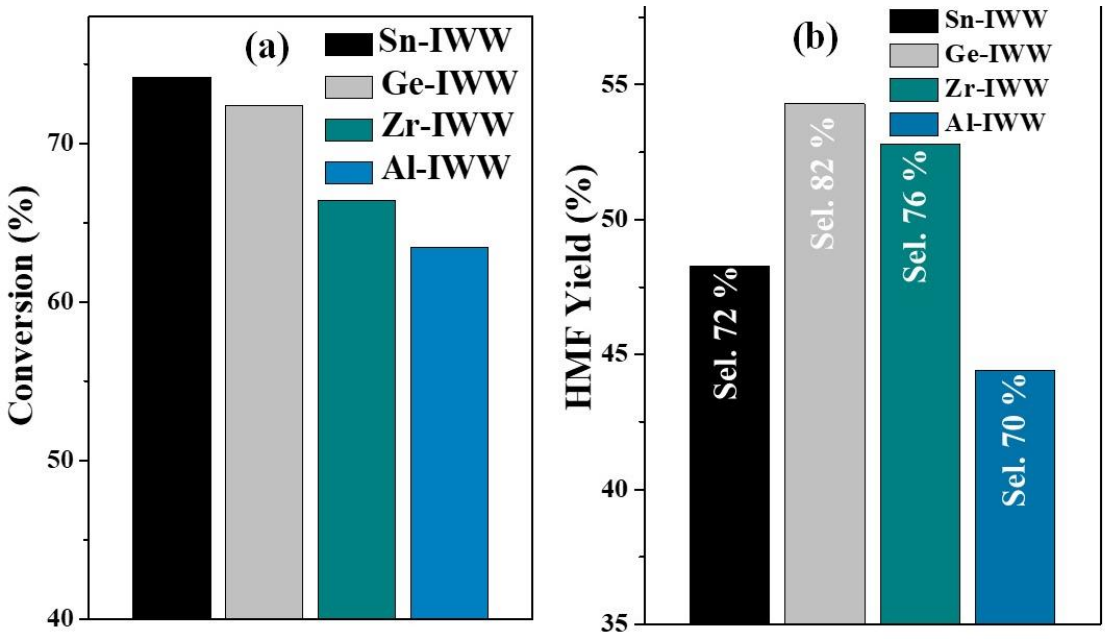

Figure 3: Sucrose conversion (a) and HMF yield (b) over the IWW zeolite catalysts under study. Reaction conditions: 1 mmol sucrose (10 wt % aqueous solution), 5 ml DMSO, 50 mg catalyst, 120 °C, 3 h.

Having detected Ge-associated acid sites that were favorable for selective sucrose-to-HMF transformation, we further assess the role of the germanosilicate zeolite catalyst structure on their catalytic behavior. Assuming diffusion limitations usually restrict the performance of microporous solid acids, Ge-UTL and Ge-*CTH zeolites with larger pores have been selected for the comparative study with Ge-IWW (Table 2). The PXRD patterns (Figure S1) reveal the structural integrity of the studied germanosilicate catalysts, and nitrogen physisorption (Figure S2) evidenced their microporous character. Extra-large pore Ge-UTL and Ge-*CTH zeolites are characterized by a 2D pore system of intersecting 14- and 12- or 14- and 10-ring pores, respectively, while Ge-IWW shows a 3D pore system of parallel 12- and 10-ring pores, which are intersected with 8-ring pores (Table 2).

Table 2: Chemical composition, textural, and catalytic properties of germanosilicate zeolite catalysts under study

Material	Si/Ge[a]	Pore rings[b]	V_{micro} ($cm^3 \cdot g^{-1}$)[c]	Crystal size (μm)	Catalytic performance (%)[d]		
					Conversion	Selectivity	Yield
Ge-IWW	5	12||10x8	0.16	<1	74	82	54
Ge-*CTH	4	14x10	0.16	30x50x<1	60	84	53
Ge-UTL	4	14x12	0.18	10x20x<1	76	85	58

[a] – based on ICP-MS analysis;
[b] – based on the International Zeolite Association Database[14];
[c] – based on nitrogen physisorption;
[d] – Reaction conditions: 1 mmol sucrose (10 wt % aqueous solution), 5 ml DMSO, 50 mg catalyst, 120 °C, 3 h.

Considering a similar chemical composition of germanosilicate zeolite catalysts, a lower conversion over Ge-*CTH can be explained by i) diffusion limitations of reagents and products in Ge-*CTH with large crystals and 2-dimensional porous system or ii) different distribution of acid sites in Ge-*CTH *vs.* Ge-UTL and Ge-IWW. The first assumption (i) was verified by SEM showing elongated crystals with rectangular morphology and size up to 10 μm for the Ge-*CTH zeolite and large rectangular crystals with average size in the range of 30 × 50 – 60 μm which are stacked with each other along a crystallographic plane for Ge-UTL (Figure S6). Therefore, despite relatively narrow pore openings (12x10x8-ring), Ge-IWW shows activity comparable to that of extra-large pore Ge-UTL, that probably related to the small size of IWW crystals and three-dimensional micropore system providing better molecular transport properties.

The second assumption (ii) was ruled out by Py-FTIR showing an increase in the number of Lewis acid sites (based on the intensity of the absorption band υ_{8a}=1611 cm^{-1}) in the following sequence of germanosilicate catalysts: Ge-UTL < Ge-*CTH < Ge-IWW (Figure S3). Notably, Py-FTIR spectra of germanosilicates showed that, the Ge-IWW zeolite contained both Lewis and Brønsted acidity, while Ge-UTL and Ge-*CTH do not contain a detectable amount of Brønsted acid centers, which were reported to facilitate the hydrolysis of sucrose to glucose and fructose as the initial step in sucrose-to-HMF transformation. However, Brønsted acidity can be introduced into germanosilicates under the reaction conditions [36]. To verify this hypothesis, the Py-FTIR study was conducted for the Ge-UTL material treated either with DMSO or with DMSO and sucrose mixture. The results showed that new bands at υ_{8a} =1637 and υ_{19b} =1545 cm^{-1} that can be assigned to Brønsted sites appeared in DMSO-treated Ge-UTL (Fig. S8), and the intensities of these bands increased after the addition of the sucrose. These results indicate that both the solvent and reactants can induce Brønsted acid sites in germanosilicates, which can facilitate the conversion of sucrose to HMF.

The reusability of germanosilicate catalysts in sucrose-to-HMF transformation was tested in 3 catalytic cycles. Although Ge-IWW and Ge-*CTH showed stable catalytic performance, the activity of Ge-UTL gradually decreased in the second and third runs (Figure 4). This behavior is explained by the worsening crystallinity of Ge-UTL under reaction conditions, as detected by XRD (Figure S8). The poor hydrolytic stability of Ge-UTL is in line with previously reported NMR spectroscopic studies [37, 38] revealing that D4R structural units in Ge-UTL zeolite framework possess four Ge atoms on the same face, making all interlayer linkages sensitive to water. On the contrary, several possible Ge arrangements in Ge-IWW and Ge-*CTH were all characterized by the presence of Si–O–Si interlayer links capable of maintaining zeolite structure against degradation by water (Figure S9).

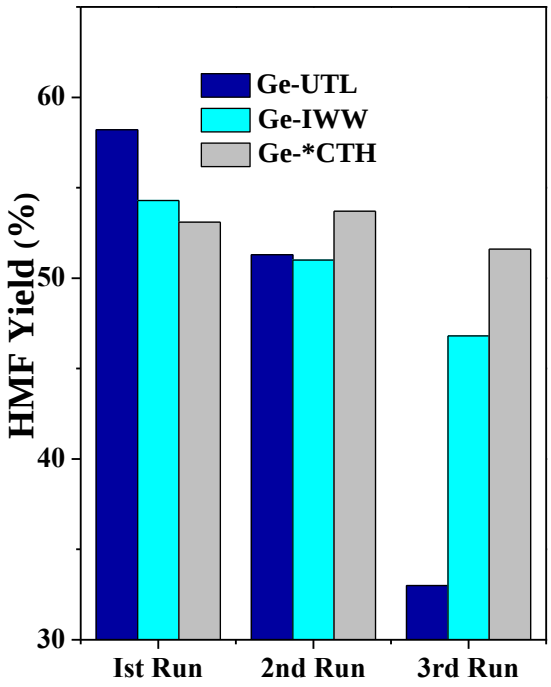

Figure 4: Reusability of the studied germanosilicate zeolite catalysts in sucrose-to-HMF transformation. Reaction conditions: 1 mmol sucrose (10 wt % aqueous solution), 5 ml DMSO, 50 mg catalyst, 120 °C, 3 h.

All in all, the results of this study reveal the strength of acid sites, pore architecture, and crystal morphology as decisive characteristics of zeolite catalysts to be optimized to maximize their activity and selectivity in the sucrose-to-HMF transformation. Germanosilicate zeolites were first shown as efficient catalysts in sucrose-to-HMF transformation, demonstrating similar conversion/selectivity values to those documented when using other homogeneous or more complex heterogeneous catalysts, such as $CrCl_3$ [39], Nb_2O_5 [40], and CeO_2-SZ@SBA-15 [41] or Cr–H-BEA [42] which provided similar performances, sometimes even at higher temperatures.

Conclusions

Large-pore IWW zeolites containing Ge, Zr, Sn, Al acid sites were designed *via* a post-synthesis degermanation/metallation approach and tested in a one-pot cascade transformation of sucrose to HMF, involving hydrolysis of sucrose to glucose and fructose over Brønsted acid sites, glucose-to-fructose isomerisation over Lewis acid sites and fructose dehydration to the targeted HMF. At moderate temperature (120 °C), the highest HMF yield (54% after 3h) was achieved using Ge-IWW. The yield of the targeted HMF decreased with increasing acid site strength due to the enhanced formation of by-products from HMF in the following sequence of the catalysts: Ge-IWW > Zr-IWW > Sn-IWW > Al-IWW.

Germanosilicate zeolites of different structures, such as Ge-UTL, Ge-*CTH, and Ge-IWW were found as active and selective catalysts in the sucrose-to-HMF transformation accompanied by the *in situ* formation of Ge Brønsted acid sites during the catalytic run. The germanosilicate crystal size, pore architecture, and Ge distribution were shown to determine the catalyst performance. The results of this study highlight zeolites with uncharacteristic chemical compositions as active, selective, and reusable catalysts for highly demanding applications in biomass valorization.

Author contributions

P.R.: Investigation (catalytic tests); Formal analysis; Writing – original draft. **J.Z.:** Investigation (synthesis of the catalysts, PXRD); Formal analysis; Writing – review & editing. **Y.Z.:** Investigation (FTIR spectroscopy); Formal analysis; Writing – review & editing. **M.O.:** Supervision; Conceptualization; Writing – review & editing. **M.S.:** Supervision; Conceptualization; Project management; Funding acquisition; Writing – review & editing. All authors contributed to the final version of the manuscript.

Conflicts of interests

There are no conflicts to declare.

Acknowledgements

This work was supported by the Ministry of Education, Youth and Sports of the Czech Republic through the ERC_CZ project LL 2104 (Y.Z., M.S., M.S.). The authors acknowledge Charles University Centre of Advanced Materials (CUCAM – OP VVV Excellent Research Teams, no. CZ.02.1.01/0.0/0.0/15_003/0000417) for providing infrastructure enabling this research. The authors thank to Dr. M. Kubů for physisorption and ICP-MS analyses and Dr. Q. Yue for acquiring SEM images.

References

[1] L.T. Mika, E. Cséfalvay, A. Németh, *Catalytic Conversion of Carbohydrates to Initial Platform Chemicals: Chemistry and Sustainability,* Chem. Rev. (Washington, DC, U. S.) 118 (2018) 505-613.

[2] C. Xu, E. Paone, D. Rodríguez-Padrón, R. Luque, F. Mauriello, *Recent catalytic routes for the preparation and the upgrading of biomass derived furfural and 5-hydroxymethylfurfural,* Chem. Soc. Rev. 49 (2020) 4273-4306.

[3] D. Hu, M. Zhang, H. Xu, Y. Wang, K. Yan, *Recent advance on the catalytic system for efficient production of biomass-derived 5-hydroxymethylfurfural,* Renew. Sust. Ener. Rev. 147 (2021) 111253.

[4] S. Kunnikuruvan, N.N. Nair, *Mechanistic Insights into the Brønsted Acid-Catalyzed Dehydration of β-d-Glucose to 5-Hydroxymethylfurfural under Ambient and Subcritical Conditions,* ACS Catal. 9 (2019) 7250-7263.

[5] D.J. Aranha, P.R. Gogate, *A Review on Green and Efficient Synthesis of 5-Hydroxymethylfurfural (HMF) and 2,5-Furandicarboxylic Acid (FDCA) from Sustainable Biomass,* Ind. Eng. Chem. Res. 62 (2023) 3053-3078.

[6] Z. Wang, S. Xia, X. Wang, Y. Fan, K. Zhao, S. Wang, Z. Zhao, A. Zheng, *Catalytic production of 5-hydroxymethylfurfural from lignocellulosic biomass: Recent advances, challenges and opportunities,* Renew. Sust. Ener. Rev. 196 (2024) 114332.

[7] E. Subbotina, A. Velty, J.S.M. Samec, A. Corma, *Zeolite-Assisted Lignin-First Fractionation of Lignocellulose: Overcoming Lignin Recondensation through Shape-Selective Catalysis,* ChemSusChem 13 (2020) 4528-4536.

[8] J. Shi, Y. Wang, W. Yang, Y. Tang, Z. Xie, *Recent advances of pore system construction in zeolite-catalyzed chemical industry processes,* Chem. Soc. Rev. 44 (2015) 8877-8903.

[9] M. Moliner, C. Martinez, A. Corma, *Multipore zeolites: synthesis and catalytic applications,* Angew. Chem. Int. Ed. 54 (2015) 3560-3579.

[10] R. Gautam, P. Pal, S. Saravanamurugan, *Enhanced Catalytic Activity of Modified ZSM-5 Towards Glucose Isomerization to Fructose,* ChemPlusChem 88 (2023) e202200299.

[11] H. Yang, Q. Guo, P. Yang, X. Liu, Y. Wang, *Synthesis of hierarchical Sn-Beta zeolite and its catalytic performance in glucose conversion,* Catal. Today 367 (2021) 117-123.

[12] E. Nikolla, Y. Román-Leshkov, M. Moliner, M.E. Davis, *"One-Pot" Synthesis of 5-(Hydroxymethyl)furfural from Carbohydrates using Tin-Beta Zeolite,* ACS Catal. 1 (2011) 408-410.

[13] P. Yan, H. Wang, Y. Liao, C. Wang, *Zeolite catalysts for the valorization of biomass into platform compounds and biochemicals/biofuels: A review,* Renew. Sust. Ener. Rev. 178 (2023) 113219.

[14] https://www.iza-structure.org/databases/.

[15] M. Shamzhy, M. Opanasenko, P. Concepción, A. Martínez, *New trends in tailoring active sites in zeolite-based catalysts,* Chem. Soc. Rev. 48 (2019) 1095-1149.

[16] M. Opanasenko, M. Shamzhy, Y. Wang, W. Yan, P. Nachtigall, J. Cejka, *Synthesis and Post-Synthesis Transformation of Germanosilicate Zeolites,* Angew. Chem. Int. Ed. 59 (2020) 19380-19389.

[17] Z.R. Gao, J. Li, C. Lin, A. Mayoral, J. Sun, M.A. Camblor, *HPM-14: A New Germanosilicate Zeolite with Interconnected Extra-Large Pores Plus Odd-Membered and Small Pores,* Angew. Chem. Int. Ed. 60 (2021) 3438-3442.

[18] H. Xu, J.G. Jiang, B. Yang, L. Zhang, M. He, P. Wu, *Post-synthesis treatment gives highly stable siliceous zeolites through the isomorphous substitution of silicon for germanium in germanosilicates,* Angew. Chem. Int. Ed. 53 (2014) 1355 –1359.
[19] M. Shamzhy, M. Opanasenko, Y. Tian, K. Konysheva, O. Shvets, R.E. Morris, J. Čejka, *Germanosilicate Precursors of ADORable Zeolites Obtained by Disassembly of ITH, ITR, and IWR Zeolites,* Chem. Mater. 26 (2014) 5789-5798.
[20] J. Zhang, O. Veselý, Z. Tošner, M. Mazur, M. Opanasenko, J. Čejka, M. Shamzhy, *Toward Controlling Disassembly Step within the ADOR Process for the Synthesis of Zeolites,* Chem. Mater. 33 (2021) 1228-1237.
[21] V. Kasneryk, M. Shamzhy, J. Zhou, Q. Yue, M. Mazur, A. Mayoral, Z. Luo, R.E. Morris, J. Cejka, M. Opanasenko, *Vapour-phase-transport rearrangement technique for the synthesis of new zeolites,* Nat. Commun. 10 (2019) 5129.
[22] M.V. Shamzhy, O.V. Shvets, M.V. Opanasenko, P.S. Yaremov, L.G. Sarkisyan, P. Chlubná, A. Zukal, V.R. Marthala, M. Hartmann, J. Čejka, *Synthesis of isomorphously substituted extra-large pore UTL zeolites,* J. Mater. Chem. 22 (2012) 15793–15803.
[23] M.V. Shamzhy, O.V. Shvets, M.V. Opanasenko, L. Kurfirtová, D. Kubicka, J. Cejka, *Extra-Large-Pore Zeolites with UTL Topology: Control of the Catalytic Activity by Variation in the Nature of the Active Sites,* ChemCatChem 5 (2013) 1891-1898.
[24] M. Shamzhy, F.S.D. Ramos, *Tuning of acidic and catalytic properties of IWR zeolite by post-synthesis incorporation of three-valent elements,* Catal. Today 243 (2015) 76-84.
[25] M.V. Shamzhy, M.V. Opanasenko, F.S.D. Ramos, L. Brabec, M. Horácek, M. Navarro-Rojas, R.E. Morris, H.D. Pastore, J. Cejka, *Post-synthesis incorporation of Al into germanosilicate ITH zeolites: the influence of treatment conditions on the acidic properties and catalytic behavior in tetrahydropyranylation,* Catal. Sci. Tech. 5 (2015) 2973-2984.
[26] V. Kasneryk, M. Opanasenko, M. Shamzhy, Z. Musilová, Y.S. Avadhut, M. Hartmann, J. Cejka, *Consecutive interlayer disassembly-reassembly during alumination of UOV zeolites: insight into the mechanism,* J. Mater. Chem. A 5 (2017) 22576-22587.
[27] A. Corma, F. Rey, S. Valencia, J.L. Jordá, J. Rius, *A zeolite with interconnected 8-, 10- and 12-ring pores and its unique catalytic selectivity,* Nat. Mater. 2 (2003) 493-497.
[28] J. Zhang, Q. Yue, M. Mazur, M. Opanasenko, M.V. Shamzhy, J. Čejka, *Selective Recovery and Recycling of Germanium for the Design of Sustainable Zeolite Catalysts,* ACS Sust. Chem. Eng. 8 (2020) 8235-8246.
[29] J.L. Paillaud, B. Harbuzaru, J. Patarin, N. Bats, *Extra-large-pore zeolites with two-dimensional channels formed by 14 and 12 rings,* Science 304 (2004) 990-992.
[30] J.H. Kang, D. Xie, S.I. Zones, S. Smeets, L.B. McCusker, M.E. Davis, *Synthesis and Characterization of CIT-13, a Germanosilicate Molecular Sieve with Extra-Large Pore Openings,* Chem. Mater. 28 (2016) 6250-6259.
[31] K.A. Cychosz, R. Guillet-Nicolas, J. García-Martínez, M. Thommes, *Recent advances in the textural characterization of hierarchically structured nanoporous materials,* Chem. Soc. Rev. 46 (2017) 389-414.
[32] I. Podolean, J. Zhang, M. Shamzhy, V.I. Pârvulescu, J. Čejka, *Solvent-free ketalization of polyols over germanosilicate zeolites: the role of the nature and strength of acid sites,* Catal. Sci. Technol. 10 (2020) 8254-8264.
[33] Z. Zhu, Y. Guan, H. Ma, H. Xu, J.-g. Jiang, H. Lü, P. Wu, *Hydrothermal synthesis of boron-free Zr-MWW and Sn-MWW zeolites as robust Lewis acid catalysts,* Chem. Commun. (Cambridge, U. K.) 56 (2020) 4696-4699.

[34] M. Shamzhy, J. Prech, J. Zhang, V. Ruaux, H. El-Siblani, S. Mintova, *Quantification of Lewis acid sites in 3D and 2D TS-1 zeolites: FTIR spectroscopic study,* Catal. Today 345 (2020) 80-87.
[35] X. Li, K. Peng, X. Liu, Q. Xia, Y. Wang, *Comprehensive Understanding of the Role of Brønsted and Lewis Acid Sites in Glucose Conversion into 5-Hydromethylfurfural,* ChemCatChem 9 (2017) 2739-2746.
[36] N. Kasian, G. Vanbutsele, K. Houthoofd, T.I. Koranyi, J.A. Martens, C.E.A. Kirschhock, *Catalytic activity and extra-large pores of germanosilicate UTL zeolite demonstrated with decane test reaction,* Catal. Sci. Technol. 1 (2011) 246–254.
[37] N. Kasian, A. Tuel, E. Verheyen, C.E.A. Kirschhock, F. Taulelle, J.A. Martens, *NMR Evidence for Specific Germanium Siting in IM-12 Zeolite,* Chem. Mater. 26 (2014) 5556-5565.
[38] X. Liu, W. Mao, J. Jiang, X. Lu, M. Peng, H. Xu, L. Han, S.-a. Che, P. Wu, *Topotactic Conversion of Alkali-Treated Intergrown Germanosilicate CIT-13 into Single-Crystalline ECNU-21 Zeolite as Shape-Selective Catalyst for Ethylene Oxide Hydration,* Chem. Eur. J. 25 (2019) 4520-4529.
[39] S. Mulk, M. Sajid, L. Wang, F. Liu, G. Pan, *Catalytic conversion of sucrose to 5-hydroxymethylfurfural in green aqueous and organic medium,* J. Env. Chem. Eng. 10 (2022) 106613.
[40] H.T. Kreissl, K. Nakagawa, Y.-K. Peng, Y. Koito, J. Zheng, S.C.E. Tsang, *Niobium oxides: Correlation of acidity with structure and catalytic performance in sucrose conversion to 5-hydroxymethylfurfural,* J. Catal. 338 (2016) 329-339.
[41] Y. Zhang, Q. Xiong, E. Zhu, M. Liu, J. Pan, Y. Yan, *Direct Conversion of C6 Monosaccharide-Based Carbohydrates to 5-Hydroxymethylfurfural by the Combination of Sulfated Zirconia and Ceria Catalysts,* Ener.Technol. 6 (2018) 1941-1950.
[42] S. Xu, D. Pan, F. Hu, Y. Wu, H. Wang, Y. Chen, H. Yuan, L. Gao, G. Xiao, *Highly efficient Cr/β zeolite catalyst for conversion of carbohydrates into 5-hydroxymethylfurfural: Characterization and performance,* Fuel Process. Technol. 190 (2019) 38-46.